

SCIENTIFIC REPORTS



OPEN

Serotonin drives the acquisition of a profibrotic and anti-inflammatory gene profile through the 5-HT7R-PKA signaling axis

Ángeles Domínguez-Soto¹, Alicia Usategui², Mateo de las Casas-Engel¹, Miriam Simón-Fuentes¹, Concha Nieto¹, Víctor D. Cuevas¹, Miguel A. Vega¹, José Luis Pablos² & Ángel L. Corbí¹

Peripheral serotonin (5-hydroxytryptamine, 5-HT) regulates cell growth and differentiation in numerous cell types through engagement of seven types of cell surface receptors (HTR1–7). Deregulated 5-HT/HTR levels contribute to pathology in chronic inflammatory diseases, with macrophages being relevant targets for the physio-pathological effects of 5-HT. In fact, 5-HT skews human macrophage polarization through engagement of 5-HT2BR and 5-HT7R receptors. We now report that 5-HT primes macrophages for reduced pro-inflammatory cytokine production and IFN type I-mediated signaling, and promotes an anti-inflammatory and pro-fibrotic gene signature in human macrophages. The acquisition of the 5-HT-dependent gene profile primarily depends on the 5-HT7R receptor and 5-HT7R-initiated PKA-dependent signaling. In line with the transcriptional results, 5-HT upregulates TGF β 1 production by human macrophages in an HTR7- and PKA-dependent manner, whereas the absence of *Htr7* *in vivo* results in diminished macrophage infiltration and collagen deposition in a mouse model of skin fibrosis. Our results indicate that the anti-inflammatory and pro-fibrotic activity of 5-HT is primarily mediated through the 5-HT7R-PKA axis, and that 5-HT7R contributes to pathology in fibrotic diseases.

Serotonin (5-hydroxytryptamine, 5-HT) is a monoamine neurotransmitter derived from L-tryptophan via a rate-limiting reaction catalyzed by tryptophan hydroxylases (TPH1 in periphery, TPH2 in brain)^{1,2}. Brain-derived 5-HT controls mood, behavior, sleep, blood pressure and thermoregulation³ whereas peripheral 5-HT regulates vascular and heart functions⁴ and gastrointestinal mobility⁵. Enterochromaffin cells in the gastrointestinal tract produce 90% of the human body's 5-HT⁶, which is actively taken up by blood platelets and stored in dense granules. Upon platelet activation, released 5-HT modifies vascular smooth muscle tone, promotes proliferation of smooth muscle cells⁷, hepatocytes⁸ and endothelial cells⁹, and critically contributes to wound healing. All 5-HT actions are exerted through engagement of seven types of receptors (5-HT1–7R) which, except for 5-HT3R, belong to the G protein-coupled superfamily of receptors¹⁰. 5-HT also functions as a regulator of immune and inflammatory responses¹¹. 5-HT modulates T-cell activation, proliferation and differentiation¹² and modifies cytokine production in a cell type-dependent manner^{13–16}. The regulatory role of 5-HT in inflammation is illustrated by the pathological consequences of its altered production or absence in chronic inflammatory diseases. 5-HT contributes to Pulmonary Arterial Hypertension (PAH)¹⁷, atopic dermatitis¹⁸ and systemic sclerosis¹⁹, and modifies the outcome of inflammatory gut disorders^{20–25}. 5-HT also favors colon cancer angiogenesis²⁶ and neuroendocrine neoplasms proliferation²⁷, and its absence increases pathologic scores in collagen-induced arthritis²⁸. The close link between 5-HT and chronic inflammatory pathologies²⁹ is in line with the anti-inflammatory actions of selective 5-HT reuptake inhibitors (SSRI) like fluoxetine^{30,31}. Further supporting the 5-HT/inflammation link, 5-HT2BR has been shown to mediate the effects of 5-HT on tissue fibrosis¹⁹ and PAH¹⁷, 5-HT7R mediates the 5-HT contribution to gut inflammation in IBD models^{20,22,23}, and 5-HT3R or 5-HT4R ligands reduce inflammatory reactions during postoperative ileus^{32,33}.

¹Myeloid Cell Laboratory, Centro de Investigaciones Biológicas, CSIC, Madrid, Spain. ²Servicio de Reumatología, Instituto de Investigación Hospital 12 de octubre, Universidad Complutense de Madrid, Madrid, Spain. Ángeles Domínguez-Soto, Alicia Usategui, Mateo de las Casas-Engel, José Luis Pablos and Ángel L. Corbí contributed equally to this work. Correspondence and requests for materials should be addressed to Á.D.-S. (email: ads@cib.csic.es)

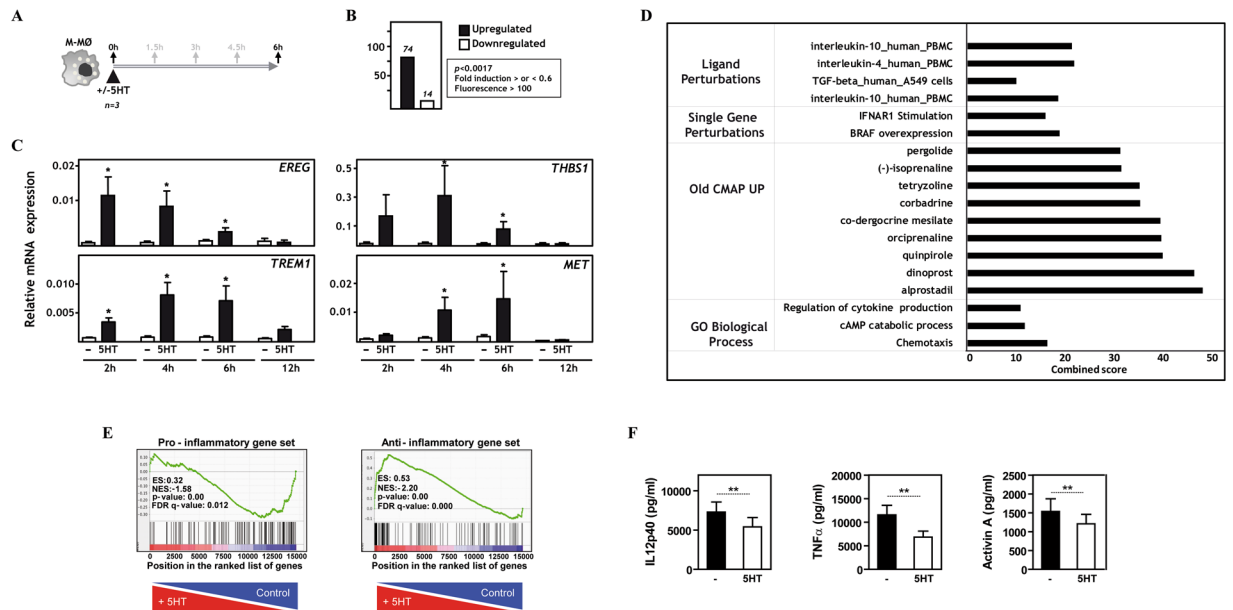


Figure 1. Serotonin promotes the acquisition of an anti-inflammatory gene profile and conditions human macrophages for diminished LPS-stimulated proinflammatory cytokine production. **(A)** Experimental design of the gene profiling experiment. **(B)** Number of annotated genes whose expression is upregulated or downregulated in M-MØ exposed to 5-HT for 6 hours ($p < 0.0017$; Upregulated, $\log_2 \text{M-MØ} + 5\text{-HT}/\text{M-MØ} > 0.6$; Downregulated, $\log_2 \text{M-MØ} + 5\text{-HT}/\text{M-MØ} < -0.6$). **(C)** Relative expression of the indicated genes in non-treated M-MØ (-) or M-MØ treated with 5-HT (5HT) for 2, 4, 6 and 12 hours. Results are expressed as the mRNA level of each gene relative to the *GAPDH* mRNA level in the same sample ($n = 3$; $*p < 0.05$). **(D)** Gene ontology analysis of the set of genes upregulated by 5-HT in M-MØ, as determined using the ENRICHR tool and the indicated databases [combined score = $\log(\text{p-value}) \times z\text{-score}$]. **(E)** GSEA on the “t statistic-ranked” list of genes obtained from the 5-HT-treated M-MØ versus M-MØ limma analysis, using the proinflammatory (left panel) and anti-inflammatory (right panel) gene sets previously defined⁴⁸. Vertical black lines indicate the position of each of the genes comprising the “Pro-inflammatory” and “Anti-inflammatory” gene sets. **(F)** Production of IL-12p40, TNF α and Activin A by non-treated (-) or 5-HT-pretreated (6 h) LPS-stimulated (18 h) M-MØ, as determined by ELISA ($n = 12$; $*p < 0.05$; $**p < 0.01$).

Macrophages are critical for maintaining tissue homeostasis and promoting the initiation and resolution of inflammatory processes. The balance between pro- and anti-inflammatory (resolving) macrophages is required for restoring tissue homeostasis^{34–36}, and its deregulation leads to chronic inflammatory diseases^{37,38}. Since macrophages rapidly adapt their functions to micro-environmental stimuli (e.g., cytokines, growth factors, pathogen- and damage-associated molecular patterns)^{34–38}, targeting macrophages is currently proposed as a therapeutic approach for chronic inflammatory diseases³⁷. Not surprisingly, some of the effects of 5-HT on inflammation are mediated through direct and indirect actions on myeloid cells^{17,26,32,33}. Further supporting this relationship, bone marrow-derived cells are responsible for the contribution of 5-HT and 5-HT7R to intestinal inflammation²², and macrophages mediate the anti-inflammatory action of SSRI^{30,39}.

We have previously demonstrated that human pro-inflammatory and anti-inflammatory macrophages^{40–43} exhibit a distinct profile of 5-HT receptors, and that 5-HT2BR and 5-HT7R shape macrophage effector functions towards the anti-inflammatory side⁴⁴. To dissect the molecular mechanisms underlying the inflammation-modulating action of 5-HT, we undertook the determination of the 5-HT-dependent transcriptome of human macrophages. 5-HT rapidly altered the human macrophage transcriptome towards a growth-promoting, anti-inflammatory and pro-fibrotic gene profile, whose acquisition was dependent on the 5-HT7R -PKA signaling axis. Moreover, and in line with these findings, *Htr7*^{-/-} mice exhibited significantly reduced macrophage accumulation and collagen deposition in a bleomycin-induced model of skin fibrosis.

Results

5-HT promotes the expression of an anti-inflammatory gene profile and inhibits pro-inflammatory cytokine production. To determine the 5HT-dependent transcriptome of human macrophages, a global gene expression analysis was performed on human monocyte-derived macrophages (M-MØ) exposed to 5-HT for 6 hours (Fig. 1A), a time at which exposure to 5-HT modifies the LPS-induced production of inflammatory cytokines (see below). Transcriptional profiling revealed that 5-HT increases the expression of 170 annotated genes ($p < 0.01$; $\log_2 \text{ratio } 5\text{-HT}/\text{untreated} \geq 0.6$) and downregulated the expression of 41 genes ($p < 0.01$; $\log_2 \text{ratio } 5\text{-HT}/\text{untreated} \leq -0.6$) (Supplementary Table I). Further filtering (normalized expression levels higher than 100 in untreated or 5-HT-treated M-MØ, and $p < 0.0017$ for the M-MØ vs. M-MØ + 5-HT comparison) identified 74 genes upregulated and 14 genes downregulated upon 5-HT exposure (Table 1) (Fig. 1B). Analysis of independent 5-HT-treated M-MØ samples confirmed the microarray data and revealed distinct kinetics for the

probeid	M-MØ	M-MØ + 5HT	log2.fold M-MØ + 5HT/M-MØ	t	pval	adj.pval	genesymbol
A_23_P19333	80.05	344.74	2.0767	16.5371	0	0.192	TREM1
A_23_P401106	154.79	2069.16	3.6833	14.6249	0	0.192	PDE2A
A_23_P416711	51.15	137.60	1.4367	14.5716	0	0.192	ST6GALNAC3
A_23_P208900	275.45	686.62	1.3333	14.3717	0	0.192	SEMA6B
A_23_P32404	410.56	963.29	1.2367	13.1219	1.0000E-04	0.2092	ISG20
A_23_P132515	102.95	300.13	1.55	12.9583	1.0000E-04	0.2092	SIDT1
A_23_P257649	331.87	745.56	1.1767	12.2964	1.0000E-04	0.2138	RBP1
A_23_P373724	55.60	115.94	1.0967	11.7738	1.0000E-04	0.2138	PPFIBP1
A_24_P49260	120.84	254.30	1.14	11.5085	1.0000E-04	0.2138	SPTLC3
A_23_P154605	3414.30	7447.51	1.1567	10.6682	2.0000E-04	0.2138	SULF2
A_23_P85453	45.04	102.33	1.2633	10.2964	2.0000E-04	0.2138	CD244
A_24_P32085	269.48	651.45	1.2633	10.2497	2.0000E-04	0.2138	MOB3B
A_33_P3352578	74.65	140.30	0.93	10.043	2.0000E-04	0.2138	CLEC4D
A_23_P321354	389.53	744.31	0.9467	10.037	2.0000E-04	0.2138	TMEM71
A_33_P3333436	78.19	169.81	1.1033	9.9911	2.0000E-04	0.2138	SGSM3
A_23_P69109	1470.47	2684.51	0.8667	9.957	2.0000E-04	0.2138	PLSCR1
A_24_P349547	218.04	750.66	1.9733	9.8847	2.0000E-04	0.2138	
A_33_P3322288	101.13	372.80	1.95	9.6901	2.0000E-04	0.2138	AZI2
A_24_P132383	491.79	927.06	0.94	9.3149	3.0000E-04	0.2138	GIMAP8
A_24_P93703	371.19	656.60	0.8167	8.9764	3.0000E-04	0.2138	TMEM198B
A_24_P324674	492.95	846.92	0.7767	8.9556	3.0000E-04	0.2138	LY9
A_23_P414654	56.39	113.19	0.9633	8.9112	3.0000E-04	0.2138	RAB37
A_24_P245379	51.84	148.73	1.4133	8.8935	3.0000E-04	0.2138	SERPINB2
A_23_P72117	446.16	1126.78	1.2967	8.8485	4.0000E-04	0.2138	SMPDL3A
A_24_P296508	702.06	1395.79	0.9533	8.7928	4.0000E-04	0.2138	SLC43A2
A_32_P161762	69.56	124.60	0.8667	8.7471	4.0000E-04	0.2138	RUNX2
A_23_P166297	227.26	450.70	0.9833	8.6544	4.0000E-04	0.2138	ABCG1
A_23_P428129	407.37	1022.43	1.32	8.6251	4.0000E-04	0.2138	CDKN1C
A_23_P102731	127.71	316.19	1.2833	8.6233	4.0000E-04	0.2138	SMOX
A_23_P404481	116.49	243.45	1.1133	8.5894	4.0000E-04	0.2138	SIPRI
A_33_P3226050	548.01	953.06	0.8	8.4776	4.0000E-04	0.2138	GATSL3
A_23_P10559	264.88	447.64	0.75	8.4521	4.0000E-04	0.2138	AATK
A_33_P3240843	170.64	314.95	0.8833	8.4384	4.0000E-04	0.2138	TMEM71
A_33_P3382560	7622.06	15383.62	1.06	8.424	4.0000E-04	0.2138	RPL23A
A_23_P25503	2952.57	6154.31	1.0633	8.4164	5.0000E-04	0.2138	FNDC3A
A_23_P86653	11484.56	19458.03	0.77	8.3019	5.0000E-04	0.2193	SRGN
A_23_P15108	532.44	913.10	0.77	8.1222	5.0000E-04	0.2193	YPEL3
A_23_P37375	217.10	359.90	0.7433	8.0574	5.0000E-04	0.2193	RPS6KA5
A_23_P89570	551.51	948.42	0.7633	8.0314	6.0000E-04	0.2193	ZMYND15
A_33_P3236177	703.17	1139.93	0.6967	7.9894	6.0000E-04	0.2193	ANG
A_23_P170453	4108.14	10205.73	1.4933	7.968	6.0000E-04	0.2193	CST5
A_33_P3273885	409.11	870.16	1.0067	7.9645	6.0000E-04	0.2193	
A_33_P3323722	2078.85	4415.23	1.0967	7.9589	6.0000E-04	0.2193	ARL4C
A_23_P59637	957.90	1874.73	0.96	7.9163	6.0000E-04	0.2193	DOCK4
A_23_P154849	87.31	145.08	0.7267	7.9088	6.0000E-04	0.2193	OLIG1
A_23_P167920	117.43	211.91	0.8467	7.7999	6.0000E-04	0.2296	DLL1
A_24_P315184	9659.77	16932.61	0.8333	7.7041	7.0000E-04	0.2387	NBEAL1
A_32_P117464	190.00	365.73	0.97	7.6492	7.0000E-04	0.2392	MB21D2
A_33_P3422294	101.01	288.34	1.4233	7.6364	7.0000E-04	0.2392	
A_33_P3317431	1153.70	2714.24	1.3067	7.5237	8.0000E-04	0.2392	
A_23_P110445	129.59	225.31	0.8067	7.5107	8.0000E-04	0.2392	APBB3
A_23_P23438	741.59	1400.56	0.9633	7.4906	8.0000E-04	0.2392	SEMA4A
A_23_P57760	101.41	159.07	0.6567	7.4768	8.0000E-04	0.2392	ACPL2
A_33_P3351775	79.06	130.10	0.6867	7.4673	8.0000E-04	0.2392	
A_33_P3227716	820.46	1369.66	0.7333	7.4591	8.0000E-04	0.2392	GATSL3

Continued

probeid	M-MØ	M-MØ + 5HT	log2.fold M-MØ + 5HT/M-MØ	t	pval	adj.pval	genesymbol
A_23_P76969	785.27	2508.70	1.6	7.4097	8.0000E-04	0.2392	SIPA1L1
A_23_P115011	59.66	102.35	0.8333	7.3499	8.0000E-04	0.2392	ADAMTSL4
A_32_P87697	29475.87	46802.86	0.6833	7.3421	8.0000E-04	0.2392	HLA-DRA
A_23_P55356	279.95	489.77	0.82	7.2414	9.0000E-04	0.2392	VMO1
A_23_P214139	349.66	647.84	0.8833	7.2258	9.0000E-04	0.2392	REV3L
A_33_P3259557	296.93	544.75	0.8333	7.1249	0.001	0.2435	TMEM198B
A_23_P79518	166.63	375.23	1.0967	7.111	0.001	0.2435	IL1B
A_24_P370172	236.53	391.70	0.72	7.0777	0.001	0.2457	LILRA5
A_23_P152791	163.03	270.51	0.75	6.851	0.0011	0.2668	SLC16A6
A_23_P400378	512.19	844.84	0.8067	6.8421	0.0011	0.2668	GPBAR1
A_23_P85716	2690.03	4201.95	0.6933	6.8414	0.0011	0.2668	FCGR2A
A_33_P3413840	121.69	228.70	0.9067	6.8214	0.0012	0.2668	GK
A_33_P3372727	54.20	141.80	1.44	6.8087	0.0012	0.2668	SEMA5A
A_23_P38795	1232.70	2077.44	0.8033	6.7376	0.0012	0.2692	FPR1
A_33_P3352098	11435.65	17831.64	0.6367	6.7192	0.0012	0.2692	MS4A7
A_33_P3315320	70.38	106.96	0.6	6.7149	0.0012	0.2692	CNTD1
A_23_P55020	656.97	1013.28	0.6133	6.659	0.0013	0.2725	CD300LF
A_33_P3415191	182.14	313.76	0.78	6.6105	0.0013	0.2733	ATP8B1
A_33_P3232557	119.84	206.66	0.7833	6.5667	0.0014	0.2733	DLGAP3
A_23_P41114	878.89	1323.40	0.6167	6.4491	0.0015	0.2733	CSTA
A_23_P201747	114.55	205.24	0.7933	6.4307	0.0015	0.2733	PADI2
A_33_P3236267	228.15	690.87	1.7367	6.4271	0.0015	0.2733	KCNQ1OT1
A_23_P380998	165.10	269.18	0.74	6.4024	0.0015	0.2733	R3HDM1
A_23_P60166	395.34	627.24	0.6367	6.3945	0.0016	0.2733	DEPTOR
A_23_P215744	91.56	144.62	0.7067	6.3883	0.0016	0.2733	CTTNBP2
A_23_P258108	11895.64	19363.83	0.7267	6.3718	0.0016	0.2733	
A_33_P3386132	397.26	623.42	0.66	6.3502	0.0016	0.2733	C2orf49
A_24_P110273	676.36	1044.92	0.6333	6.3217	0.0016	0.2733	
A_23_P25566	4726.99	7713.17	0.7067	6.3212	0.0016	0.2733	GPR183
A_23_P67896	269.49	137.51	-0.9233	-6.3894	0.0016	0.2733	SCN3A
A_23_P125204	492.06	317.00	-0.6133	-6.4729	0.0015	0.2733	OR10G8
A_33_P3232955	920.03	555.00	-0.77	-6.662	0.0013	0.2725	F2RL3
A_32_P134290	1591.48	1022.82	-0.65	-6.7639	0.0012	0.2689	ZCCHC2
A_23_P62967	1743.65	1144.21	-0.6033	-6.7737	0.0012	0.2689	DISC1
A_33_P3512350	675.48	399.65	-0.7567	-6.9789	0.0011	0.2531	LOC339807
A_23_P340848	1536.35	979.80	-0.6667	-7.0574	0.001	0.246	PTGIR
A_23_P103034	214.84	114.56	-0.9067	-7.2742	9.0000E-04	0.2392	CRYBA4
A_23_P328545	440.40	259.98	-0.7633	-8.0807	5.0000E-04	0.2193	GABRP
A_23_P404162	100.99	46.26	-1.0767	-8.2829	5.0000E-04	0.2193	HDAC9
A_23_P81441	1493.93	874.24	-0.76	-8.7105	4.0000E-04	0.2138	C5orf20
A_33_P3380383	4374.93	2579.19	-0.8067	-8.8739	4.0000E-04	0.2138	TIFAB
A_23_P91095	523.44	291.00	-0.8367	-9.6298	2.0000E-04	0.2138	CD28
A_32_P155666	716.76	350.13	-1.0733	-9.703	2.0000E-04	0.2138	ECEL1

Table 1. Gene expression analysis on untreated (M-MØ) and 5-HT-treated (10 µM, 6h) M-MØ (M-MØ+5HT), where the normalized fluorescence of each probe (*probeid*) and the corresponding gene symbol (*genesymbol*) is indicated. Probes are ordered according to the t-value (*t*) of the M-MØ+5HT/ M-MØ ratio, and the p values obtained after adjusting for multiple hypotheses testing (*adj.pval*) are shown.

5-HT-upregulated genes. As shown in Fig. 1C, *EREG* expression was maximally upregulated only two hours after exposure to 5-HT, while other genes (*TREM1*, *MET*, *THBS1*) exhibited maximal level of up-regulation 4–6 hours after 5-HT treatment. Therefore, 5-HT modifies the gene signature of human macrophages and its effects can be detected as early as 2 hours after exposure to the neurotransmitter.

Gene ontology analysis supported the relevance of the transcriptomic data because the 5-HT-upregulated gene set included a significant percentage of genes whose expression is increased by serotonin receptors agonists like co-dergocrine mesilate ($adj\ p = 2.9 \times 10^{-10}$) and pergolide ($adj\ p = 3.03 \times 10^{-8}$) (Fig. 1D). In fact, pergolide is an agonist for 5-HT₂BR that causes valvular heart disease^{45,46} and M-MØ express functional 5-HT₂BR receptors⁴⁴. Besides, 5-HT enhanced the expression of genes positively regulated by prostaglandins (Alprostadil, Dinoprost),

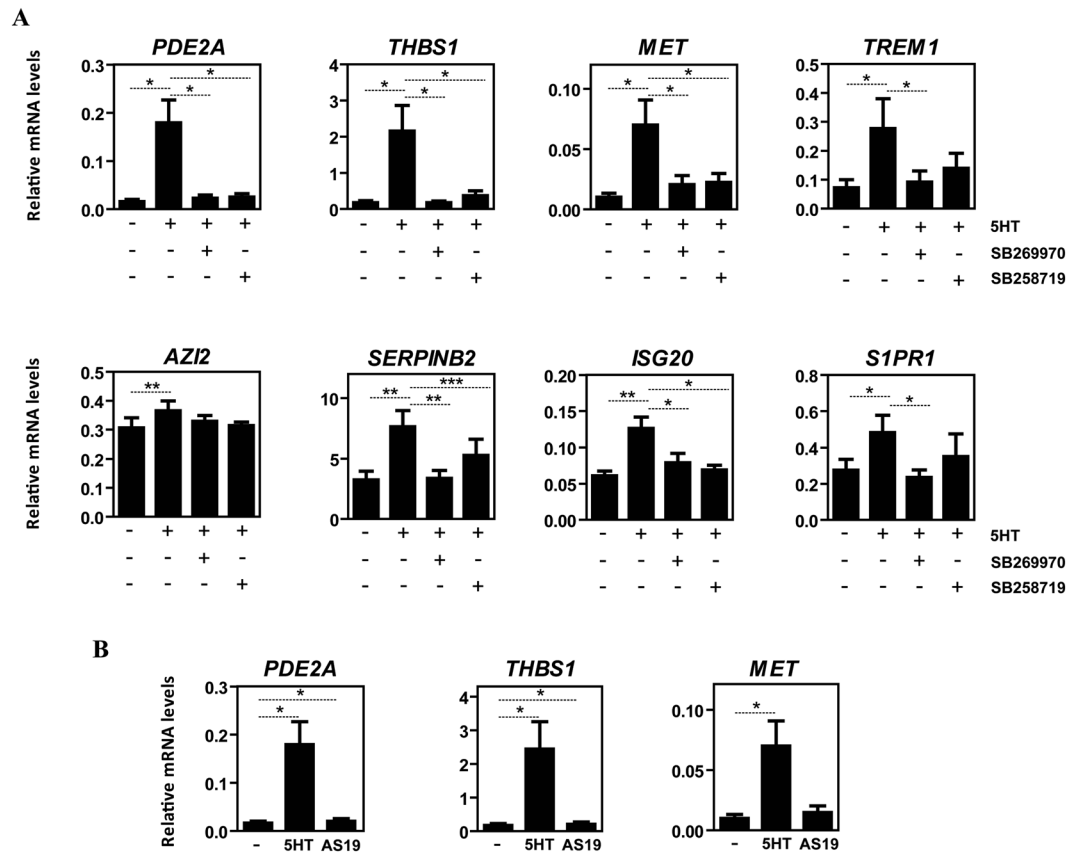


Figure 2. The acquisition of the 5-HT-dependent gene signature of human M-MØ is mediated by the 5-HT7R receptor. **(A)** Relative expression of the indicated genes in non-treated (-) or 5-HT-treated (5HT, 6h) M-MØ and either in the absence (-) or in the presence of the 5-HT7R antagonists SB269970 or SB258719. Results are expressed as the mRNA level of each gene relative to the *TBP* mRNA level in the same sample ($n = 6$; * $p < 0.05$; ** $p < 0.01$; *** $p < 0.001$). **(B)** Relative expression of the indicated genes in M-MØ either non-treated (-) or treated for 6h with 5-HT or the 5-HT7R agonist AS19. Results are expressed as the mRNA level of each gene relative to the *TBP* mRNA level in the same sample ($n = 6$; * $p < 0.05$).

dopamine (Quinpirole, co-dergocrine mesilate), and adrenergic (Orciprenaline, Tetryzoline, (-)-isoprenaline) receptor ligands (Fig. 1D). Regarding biological processes, gene ontology analysis revealed that 5-HT-upregulated genes are significantly enriched in genes involved in chemotaxis (adj $p = 1.8 \times 10^{-3}$), cAMP catabolic process (adj $p = 1.3 \times 10^{-2}$) and regulation of cytokine production (adj $p = 1.7 \times 10^{-2}$), as well as in genes regulated by IL-10 (adj $p = 8.3 \times 10^{-6}$ and adj $p = 4.2 \times 10^{-5}$) and TGF β (adj $p = 2.7 \times 10^{-3}$), and negatively regulated upon IFNAR1 stimulation (adj $p = 7.0 \times 10^{-5}$) (Fig. 1D).

The availability of the 5-HT-dependent transcriptome in M-MØ allowed us to address the global effect of 5-HT on the macrophage transcriptome. We have previously determined the gene expression profiles of IL-10-producing anti-inflammatory (M-MØ) and TNF- α -producing pro-inflammatory (GM-MØ) human macrophages⁴⁷⁻⁴⁹, and identified two sets of 150 genes that best define their corresponding transcriptomes (“Anti-inflammatory gene set” for M-MØ, and “Pro-inflammatory gene set” for GM-MØ)^{47,48}. Analysis of the expression of both gene sets in 5-HT-treated macrophages using Gene Set Enrichment Analysis (GSEA) revealed that, compared to untreated cells, the transcriptome of 5-HT-treated macrophages shows a significantly higher expression of the “Anti-inflammatory gene set” (FDR q value = 0.000) together with a significantly lower expression of the “Pro-inflammatory gene set” (FDR q value = 0.012) (Fig. 1E). In fact, genes within the leading edge of the “anti-inflammatory gene set” included *CD163L1*, *HTR2B*, and *IL10*, whose expression is closely linked to M-CSF-driven anti-inflammatory polarization^{44,48,49} (Fig. 1E, right panel and data not shown). At the functional level, and in line with GSEA results, 5-HT pretreatment (6 hours) led to a significant reduction in the LPS-induced production of IL-12p40, TNF α and Activin A of M-MØ (Fig. 1F). Therefore, 5-HT promotes the acquisition of an anti-inflammatory gene profile and conditions macrophages for a diminished pro-inflammatory response towards pathogenic stimuli.

5-HT modulates macrophage transcriptome and function primarily via the 5-HT7R-PKA signaling axis. To determine the receptors responsible for the acquisition of the 5HT-dependent transcriptional and functional profile in 5-HT7R⁺/5-HT2BR⁺ M-MØ⁴⁴, macrophages were exposed to 5-HT in the presence of 5-HT7R antagonists SB269970⁵⁰ or SB258719⁵¹, or the 5-HT2BR antagonist SB204741⁵². Whereas blockade of 5-HT2BR had no effect (Supplementary Figure 1), 5-HT7R antagonists prevented or significantly inhibited the

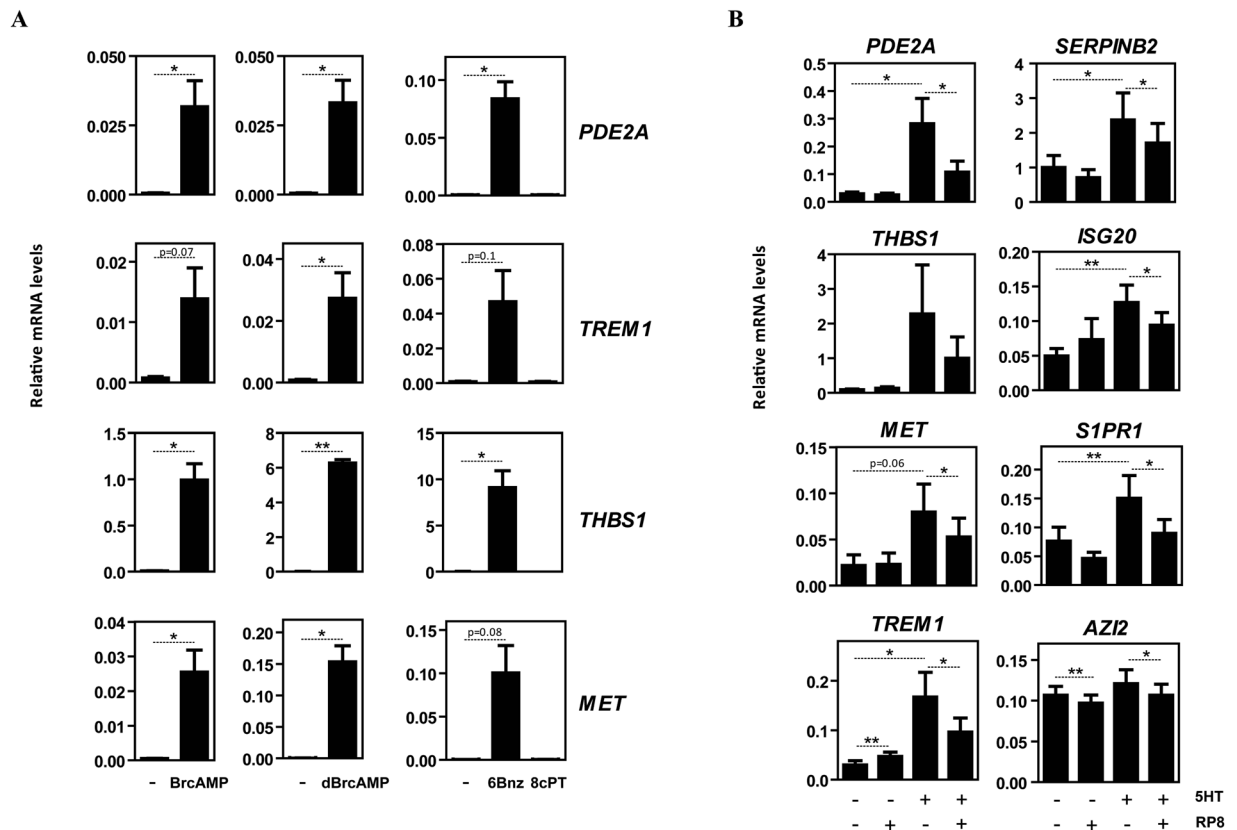


Figure 3. The acquisition of the 5-HT/5-HT7R-dependent gene signature of human M-MØ is mediated by PKA. **(A)** Relative expression of the indicated genes in M-MØ either untreated (-) or treated for 6 h to the PKA activators BrcAMP, dBrcAMP or 6Bnz, or to the Epac activator 8cPT. Results are expressed as the mRNA level of each gene relative to the *GAPDH* mRNA level in the same sample ($n = 3$; * $p < 0.05$). **(B)** Relative expression of the indicated genes in non-treated (-) or 5-HT-treated (5HT, 6 h) M-MØ and either in the absence (-) or in the presence of the PKA inhibitor RP8. Results are expressed as the mRNA level of each gene relative to the *TBP* mRNA level in the same sample ($n = 6$; * $p < 0.05$; ** $p < 0.01$).

5-HT-dependent up-regulation of *PDE2A*, *THBS1*, *MET*, *TREM1*, *SERPINB2*, *ISG20*, *AZI2* and *S1PR1* (Fig. 2A). Although to a lower extent than 5-HT, the 5-HT7R agonist AS19 was capable of enhancing the expression of *PDE2A* and *THBS1* (Fig. 2B), further supporting the involvement of 5-HT7R in the 5-HT-dependent gene expression changes in human macrophages. However, since AS19 had no effect on other 5-HT-regulated genes (*MET*) (Fig. 2B), additional receptors might also contribute to the acquisition of the 5-HT-dependent gene signature.

Since 5-HT7R engagement leads to increased intracellular levels of cAMP⁵³, whose effectors include PKA and “Exchange factor directly activated by cAMP” (Epac), we next assessed the effect of cAMP analogs (BrcAMP, dBrcAMP) and modifiers of cAMP-initiated signaling (6Bnz, 8cPT, RP8) on the acquisition of the 5-HT-dependent gene signature in M-MØ. The cAMP analogs BrcAMP and dBrcAMP greatly enhanced the expression of genes upregulated by 5-HT (*PDE2A*, *TREM1*, *THBS1*, *MET*) (Fig. 3A). Similar changes in the expression of these genes were seen in M-MØ exposed to the PKA-specific activator 6-Bnz-cAMP (Fig. 3A), while the Epac activator 8-pCPT had no effect (Fig. 3A). Moreover, the positive effect of 5-HT on the expression of 5-HT-upregulated genes was significantly blunted or inhibited in the presence of the PKA inhibitor RP8 (Fig. 3B). Therefore, 5-HT shapes M-MØ gene expression primarily via engagement of 5-HT7R and activation of PKA.

Since the 5-HT7R-PKA axis mediates the expression of the 5-HT-dependent M-MØ transcriptome, we next evaluated whether this signaling axis contributes to the inhibitory effect of 5-HT on the LPS-induced production of inflammatory cytokines by M-MØ, which produce undetectable levels of TNF α and IL-12p40 in the absence of stimulation⁴⁴. Both 5-HT7R antagonists (SB269970 and SB258719) dose-dependently reversed the inhibitory action of 5-HT on the production of TNF α and IL-12p40 induced by LPS (Fig. 4A), while the 5-HT7R agonist AS19 (1 μ M) mimicked the effect of 5-HT on the LPS-induced expression of TNF α and IL-12p40 (Fig. 4B). Furthermore, the inhibitory effect of 5-HT on the LPS-induced production of TNF α and IL-12p40 was significantly reduced in the presence of the PKA inhibitor RP8 (Fig. 4C). Thus, 5-HT conditions macrophages for a diminished production of pro-inflammatory cytokines primarily via engagement of 5-HT7R and activation of PKA. As a whole, this set of results demonstrates that the 5-HT7R-PKA axis mediates the acquisition of the 5-HT-dependent gene and cytokine profile in human macrophages.

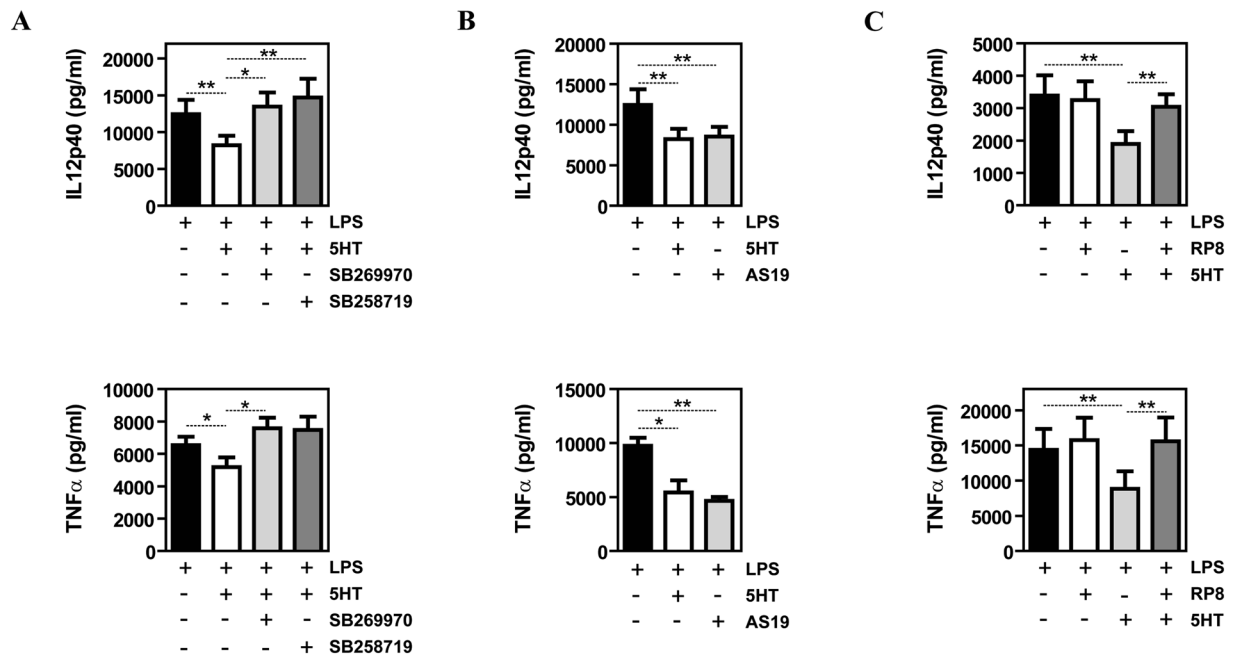


Figure 4. The inhibitory effect of 5-HT on the LPS-induced pro-inflammatory cytokine production of human macrophages is dependent on 5-HT7R and PKA. **(A)** Production of LPS-stimulated IL-12p40 and TNF α by M-M ϕ non-treated (-) or pretreated with 5-HT (6 h) in the presence or absence of the 5-HT7R antagonists SB269970 or SB258719 (n = 6; *p < 0.05; **p < 0.01; ***p < 0.001). **(B)** Production of LPS-stimulated IL-12p40 and TNF α by M-M ϕ non-treated (-) or pretreated (6 h) with either 5-HT (5HT) or the 5-HT7R agonist AS19 (n = 6; *p < 0.05; **p < 0.01). **(C)** Production of LPS-stimulated IL-12p40 and TNF α by M-M ϕ non-treated (-) or pretreated with 5-HT (5HT, 6 h) in the presence or absence of the PKA inhibitor RP8 (n = 6; *p < 0.05; **p < 0.01).

5-HT impairs type I IFN-dependent gene and chemokine expression through the 5-HT7R-PKA axis. To gain further biological insights from the 5-HT-dependent M-M ϕ transcriptome, we performed GSEA on the 5-HT-induced gene profile using gene sets contained in the Molecular Signature databases available at the GSEA Website. GSEA on the 5-HT-dependent transcriptome using the gene sets revealed a significant enrichment of the “hallmark IFN γ response” (FDR q value = 0.102) and “hallmark IFN α response” (FDR q value = 0.187) gene sets within the genes upregulated by 5-HT (Fig. 5A). In agreement with the GSEA data, the mRNA levels of type I IFN-dependent genes (*CXCL10*, *CXCL11*, *IDO1*, *RSAD2*, *IL27* and *IFIT2*) (Fig. 5B) and the production of the type I IFN-dependent chemokine CXCL10 (Fig. 5C) were significantly reduced in LPS-treated M-M ϕ that had been pre-treated for 6 hours with 5-HT. Moreover, M-M ϕ also produced reduced levels of CXCL10 in response to IFN β if previously exposed to 5-HT (Fig. 5D). The decrease in LPS- or IFN β -induced CXCL10 production caused by 5-HT exposure correlated with a reduced activation of STAT1 in response to either LPS or IFN β (Fig. 5E,F), further supporting the 5-HT’s ability to limit macrophage responses to type I IFN. Importantly, the ability of 5-HT to limit the expression of type I IFN-responsive genes is also mediated by the 5-HT7R-PKA axis, as it was abolished by either 5-HT7R antagonists (SB269970 and SB258719) or the PKA inhibitor RP8 (Fig. 5G).

5-HT also promotes pro-fibrotic gene expression in human macrophages. Additional GSEA results evidenced that a short-term (6 h) exposure to 5-HT causes a global upregulation of the “Angiogenesis” gene sets, as well as a very significant downregulation of the “Cholesterol homeostasis” and “Fatty Acid Metabolism” genes sets (Supplementary Figure 2). Furthermore, 5-HT treatment led to a significant upregulation of the “TGF β signaling” gene set (FDR q-val = 0.126) (Fig. 6A). In line with the GSEA data, 5-HT was found to induce a significant increase in *TGF β 1* mRNA (Fig. 6B). Like most 5-HT-upregulated genes, the enhanced expression of *TGF β 1* mRNA was prevented by 5-HT7R antagonists (Fig. 6B) and did not occur in the presence of the PKA inhibitor RP8 (Fig. 6C). More importantly, 5-HT treatment of M-M ϕ resulted in a significantly increase production of TGF β 1 (Fig. 6D). Therefore, engagement of 5-HT7R by 5-HT promotes the production of TGF β 1 as well as the acquisition of a pro-fibrotic gene signature in human macrophages.

Lack of *Htr7* results in diminished macrophage infiltration and pathology in a mouse model of skin fibrosis. Macrophages exert critical functions during tissue repair after injury but their deregulated polarization can also result in excessive scarring and chronic fibrosis^{54,55}. In fact, macrophages are important cells for the onset of scleroderma^{56,57} and pulmonary fibrosis^{58,59}, and their deregulated polarization results in fibrosis in muscle⁶⁰. Given the 5-HT/5-HT7R-upregulated expression of TGF β 1 in human macrophages, and to analyze the contribution of 5-HT7R to skin fibrosis development, we assessed the effect of *Htr7* gene ablation in the

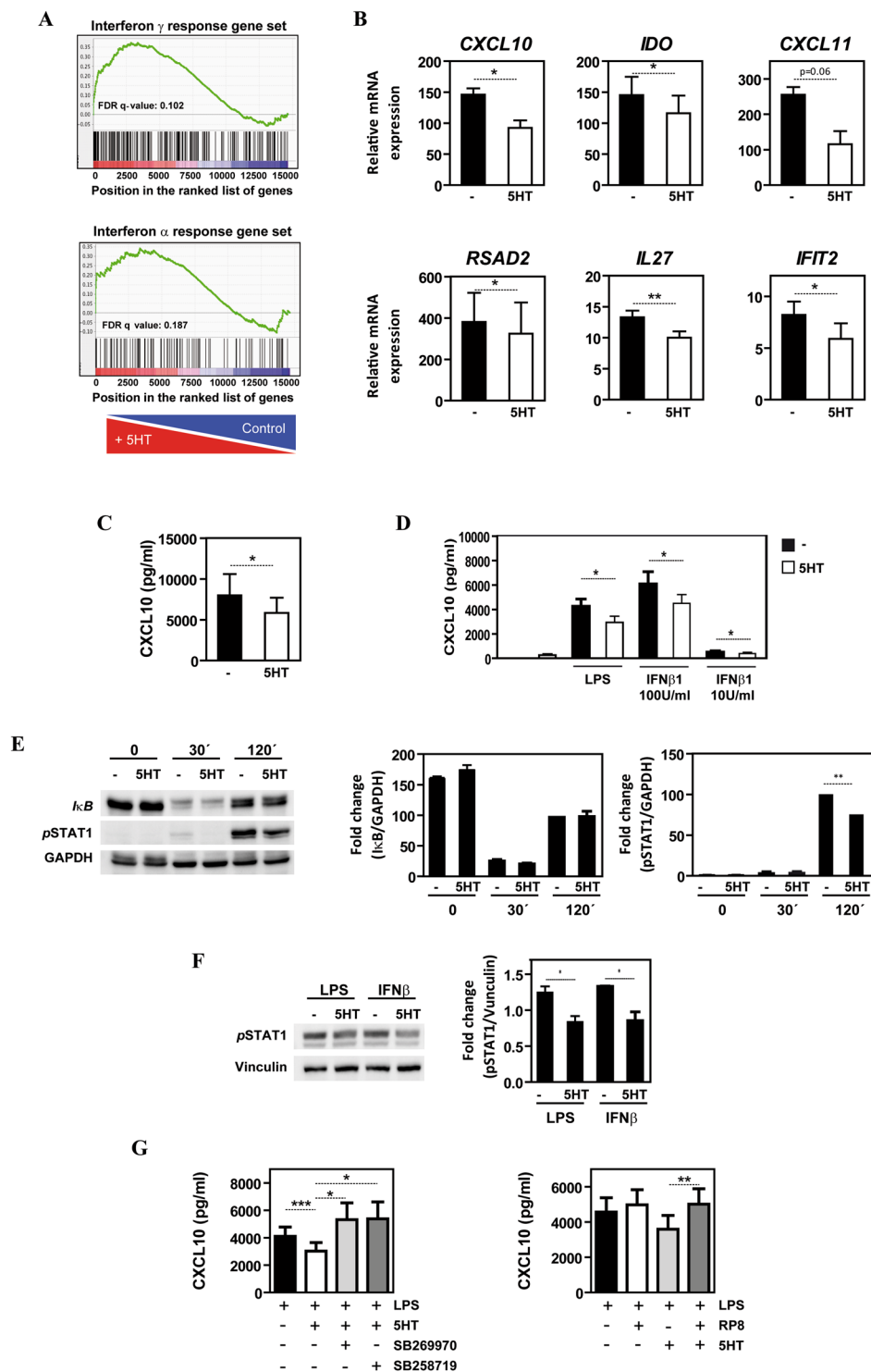


Figure 5. Serotonin modifies the type I IFN-dependent gene profile and impairs the response of human macrophages to type I IFN through 5-HT₇R and PKA. **(A)** GSEA on the “t statistic-ranked” list of genes obtained from the 5-HT-treated M-MØ versus M-MØ limma analysis, using the “Hallmark_Interferon_gamma_response” (left panel) and the “Hallmark_Interferon_alpha_response” (right panel) gene sets. **(B)** Expression of the indicated genes in untreated (-) or 5-HT-pretreated (5HT, 6 h) LPS-stimulated (4 h) M-MØ, as determined by qRT-PCR. Results are expressed as the mRNA level of each gene relative to the level of *TBP* mRNA in the same sample ($n = 3$; $*p < 0.05$; $**p < 0.01$). **(C)** Production of LPS-stimulated CXCL10 by untreated (-) M-MØ and 5-HT-treated M-MØ (5HT, 6 h) exposed to LPS for 18 h ($n = 12$; $*p < 0.05$). **(D)** Production of IFN β 1-stimulated CXCL10 by M-MØ non-treated (-) or pretreated with 5-HT (5HT, 6 h), using the indicated concentrations of IFN β 1 ($n = 13$; $*p < 0.05$). **(E)** Levels of I κ B α and phosphorylated STAT1 in untreated (-) M-MØ and 5-HT-treated M-MØ (5HT, 6 h), after stimulation with LPS for the indicated periods of time (left panel). Protein loading was normalized using a monoclonal antibody against GAPDH.

Densitometric analysis of three independent experiments is shown in the right panels ($n = 3$; $**p < 0.01$). (F) Levels of phosphorylated STAT1 in untreated (-) M-MØ and 5-HT-treated M-MØ (5HT, 6 h), after stimulation with LPS or IFN β 1 (for 2 h). Protein loading was normalized using a monoclonal antibody against Vinculin. Densitometric analysis of three independent experiments is shown in the right panels ($n = 3$; $*p < 0.05$). (G) Production of LPS-stimulated CXCL10 by non-treated (-) M-MØ or M-MØ pretreated with 5-HT (5HT, 6 h) in the presence or absence of the 5-HT7R antagonists SB269970 or SB258719 ($n = 6$; $*p < 0.05$; $***p < 0.001$) (left panel) or in the presence or absence of the PKA inhibitor RP8 ($n = 6$; $**p < 0.01$) (right panel).

mouse model of bleomycin-induced dermal fibrosis that mimics histological features of human scleroderma⁶¹. To this end we first determined *Htr7* expression of in mouse macrophages *in vitro* and *in vivo*. *Htr7* mRNA was readily detected in liver Kupffer cells and peritoneal F4/80⁺ macrophages, with *Htr7a* being the predominant splicing isoform in both cases (Supplementary Figure 3A). Unlike human monocyte-derived macrophages, *Htr7* mRNA was only detected in murine pro-inflammatory GM-MØ, where also *Htr7a* was the predominant isoform (Supplementary Figure 3B). Also in marked contrast with human macrophages, where *HTR7* mRNA is greatly reduced in response to LPS⁴⁴, macrophage *Htr7* mRNA was greatly upregulated after LPS stimulation (Supplementary Figure 3C).

Once the presence of *Htr7* mRNA had been demonstrated in murine macrophages, the effect of *Htr7* gene deletion in a mouse model of fibrosis was assessed. Whereas no histological differences in collagen stained area were observed between saline-treated *Htr7*^{-/-} and WT mice, a significant increase in skin collagen content was observed after bleomycin injection in WT mice (Fig. 6E). Conversely, *Htr7*^{-/-} mice appeared protected from bleomycin-induced fibrosis since significantly reduced collagen area content was observed in bleomycin-treated *Htr7*^{-/-} skin compared to WT skin (Fig. 6E). In addition, myofibroblast differentiation evaluated as α -SMA expression, was also significantly reduced in *Htr7*^{-/-} compared to WT mice (Fig. 6E). Likewise, a significantly lower infiltration of F4/80⁺ cells was found in bleomycin-treated *Htr7*^{-/-} mice (Fig. 6E). In addition, bleomycin treatment significantly enhanced α -SMA expression in WT mice but not in *Htr7*^{-/-} mice (Fig. 6E). Therefore, and in line with the transcriptional results in human macrophages, 5-HT7R expression contributes to macrophage accumulation and fibrosis in the bleomycin model of skin fibrosis.

Discussion

Macrophages exhibit a huge phenotypic and functional heterogeneity, and their effector functions (“polarization state”) are determined by the integration of the intracellular signals initiated by the surrounding extracellular cues and stimuli. Elimination of inflammatory insults requires the balanced and sequential dominance of pro-inflammatory and anti-inflammatory/resolving macrophages⁶² whose deregulation leads to chronic inflammatory diseases^{63–65}. Given their critical role in the initiation and resolution of inflammation, modulation of the macrophage polarization state has been proposed as a therapeutic approach for numerous chronic inflammatory pathologies³⁷. While the physiological processes regulated by 5-HT (cell proliferation, tissue repair, inflammation) are also critically modulated by macrophages⁶⁶, the influence of 5-HT on macrophage plasticity is not yet completely understood¹¹. Based on the ability of 5-HT to modulate the macrophage cytokine profile⁴⁴, we undertook the determination of the 5-HT-dependent human macrophage transcriptome. Our results indicate that 5-HT conditions macrophages for impaired production of pro-inflammatory cytokines and type I IFN-inducible cytokines, and also shapes the macrophage gene signature towards the acquisition of an anti-inflammatory and pro-fibrotic gene profile, with all these effects being primarily mediated by the 5-HT7R-PKA axis.

The link between 5-HT and fibroblast proliferation/fibrosis has been known to be primarily mediated by the 5-HT2BR receptor, which induces extra-cellular matrix synthesis in fibroblasts¹⁹ and whose over-activation leads to excessive proliferation of cardiac valves fibroblasts and severe cardiac pathologies^{67–69}. Our results reveal that 5-HT7R is a primary mediator of the pro-fibrotic action of 5-HT on human macrophages because 5-HT7R antagonists and inhibitors of 5-HT7R-initiated signaling block the acquisition of the pro-fibrotic gene signature as well as the 5-HT-upregulated production of TGF β 1 in human macrophages. The pro-fibrotic action of 5-HT7R is further supported by *in vivo* results, as *Htr7*^{-/-} mice exhibit diminished pathology (lower collagen deposition and F4/80⁺ cell infiltration) in the bleomycin-induced model of skin fibrosis. Macrophages play a critical role in fibrotic processes⁵⁴. In fact, elimination of macrophages expressing Fcrl2, a myeloid-specific protein exclusively expressed by anti-inflammatory M-MØ⁷⁰, greatly diminishes pathology in the bleomycin-induced experimental skin fibrosis⁷¹. Therefore, it can be speculated that the absence of 5-HT7R in mouse macrophages contributes to the diminished skin pathology we have observed. Alternatively, other macrophage 5-HT7R-dependent functions might contribute to the reduced pathology seen in *Htr7*^{-/-} mice. Specifically, impaired migration of myeloid cells to the bleomycin-treated tissue might explain the reduced accumulation of F4/80⁺ cells in the damaged skin of *Htr7*^{-/-} mice. This explanation would fit with the impaired migration of mouse bone marrow-derived dendritic cells from *Htr7*^{-/-} mice⁷² and is supported by the significant 5-HT-dependent upregulation of genes involved in cell chemotaxis (Fig. 1D). However, these interpretations should be taken cautiously, because expression of 5-HT7R appears to be differentially regulated in mouse and human macrophages: 5-HT7R in human macrophages is greatly downregulated by pathogenic stimuli like LPS⁴⁴ whereas *Htr7* expression in mouse myeloid cells is greatly upregulated by LPS⁷². In line with our findings, the 5-HT7R agonist LP-44 has been reported to reduce pro-inflammatory cytokine production *in vivo* in a carbon tetrachloride-induced rat model of liver fibrosis⁷³, where the agonist was, however, also capable of inhibiting *Tgfb1* mRNA⁷³. The latter discrepancy between these results and ours might be explained by the use of different 5-HT7R agonists (5HT versus a chemical agonist) and animal models of fibrosis (bleomycin-induced mouse skin fibrosis versus carbon tetrachloride-induced rat liver fibrosis), but indicate a significant involvement of 5-HT7R in fibrotic responses.

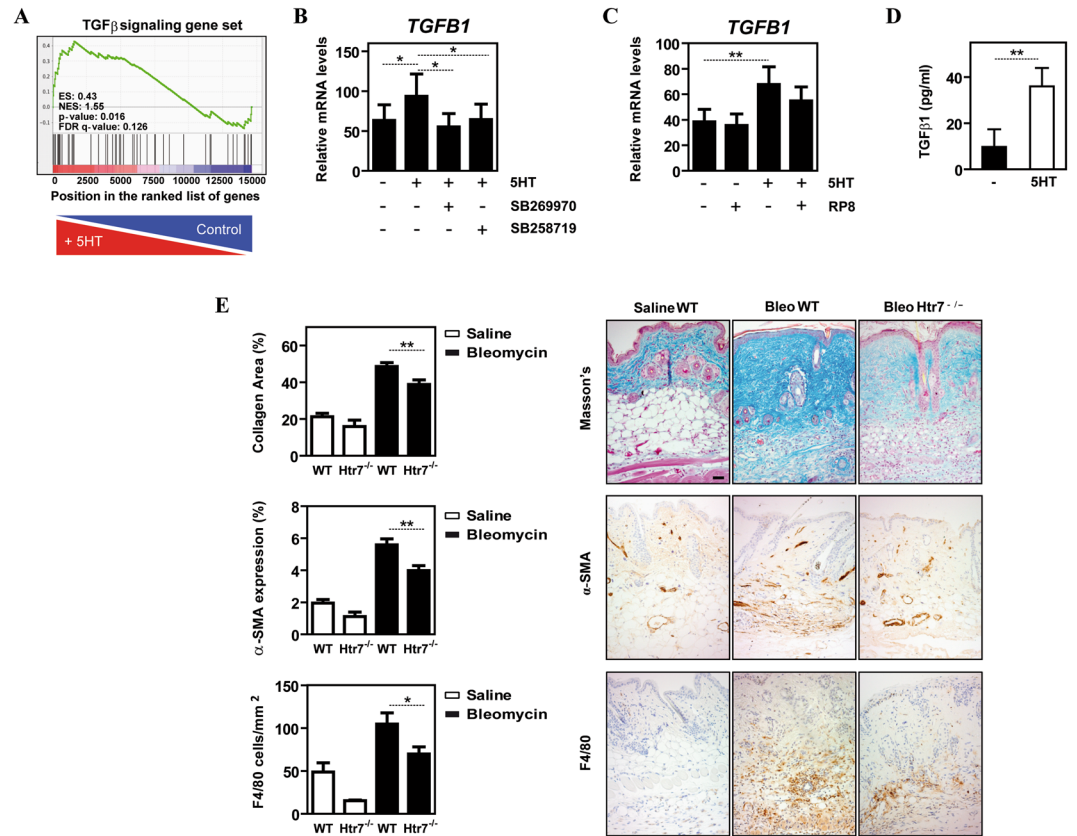


Figure 6. 5-HT7R engagement promotes the acquisition of a pro-fibrotic gene signature in human macrophages and contributes to pathology-associated parameters in a mouse model of skin fibrosis. (A) GSEA on the “t statistic-ranked” list of genes obtained from the 5-HT-treated M-MØ versus M-MØ limma analysis, using the “TGF β signaling” gene set. Black vertical lines indicate the position of each of the genes included within the “TGF β signaling” Hallmark gene set. (B) Relative expression of *TGF β 1* mRNA in non-treated M-MØ (-) or M-MØ exposed to 5-HT (5HT, 6 h) in the absence or in the presence of the 5-HT7R antagonists SB269970 or SB258719. Results are expressed as the *TGF β 1* mRNA level relative to the *TBP* mRNA level in the same sample (n = 6; *p < 0.05). (C) Relative expression of *TGF β 1* mRNA in non-treated M-MØ (-) or M-MØ exposed to 5-HT (5HT, 6 h) in the absence or in the presence of the PKA inhibitor RP8. Results are expressed as the *TGF β 1* mRNA level relative to the *TBP* and *HPRT1* mRNA level in the same sample (n = 6; *p < 0.05; **p < 0.01). (D) Production of TGF β 1 by non-treated M-MØ (-) or M-MØ treated with 5-HT (5HT) for 24 h. (n = 3; **p < 0.01). (E) Fibrosis was measured as the collagen Masson stained area (upper panel), immunohistochemistry analysis of activated fibroblasts (α -SMA⁺, middle panel), and number of F4/80⁺ cells per area (lower panel), in lesional skin from saline- or bleomycin-treated control and *Htr7*^{-/-} mice. Shown are the mean and SEM of three independent experiments with 10 mice per group. Statistical significance was evaluated using Mann-Whitney U-test, (*p < 0.05; **p < 0.01). Representative skin sections stained are shown (bar, 50 μ M).

In peripheral tissues, 5-HT7R is expressed in smooth muscle cells of blood vessels and the gastrointestinal tract, as well as in kidney, liver, pancreas and spleen^{74–76}. Within the immune system, the functional consequences of 5-HT7R ligation are far from clear. 5-HT7R on mouse naive T cells contributes to early T-cell activation¹², whereas 5-HT7R on human monocytes has been reported to inhibit⁷⁷ or enhance⁷⁸ LPS-induced pro-inflammatory cytokine release. A similar controversy appears to exist regarding the *in vivo* role of *Htr7*, whose deletion has been reported to improve²² or exacerbate²³ mouse gut inflammation. Our transcriptional results clarify this issue and demonstrate that 5-HT7R, acting through PKA, conditions macrophages towards the acquisition of a more anti-inflammatory and pro-fibrotic polarization state and for an impaired production of pro-inflammatory functions. As a consequence, our results place 5-HT7R as a potentially relevant molecule for modulation of macrophage effector functions under physiological and pathological settings.

The anti-inflammatory gene profile promoted by 5-HT/5-HT7R is compatible with the known signaling ability of 5-HT7R. Although 5-HT7R has been shown to activate NF κ B in monocytes^{12,78}, and ERK1/2⁷⁹, Akt⁸⁰, p38MAPK and protein kinase C ϵ ⁸¹, or the Cdc42-G α 12-SRF axis⁸² in various cell types, 5-HT7R couples positively to adenylate cyclase through activating G α s, leading to increased cAMP levels and activation of PKA and Epac1/2⁷⁴. These cell-specific differences in 5-HT7R signaling might derive from the presence of distinct splicing isoforms or heterodimerization with other receptors^{83,84}. In the case of human macrophages, where the three splicing isoforms can be detected at the mRNA level (data not shown), our results clearly establish PKA, and not

Epac1/2, as a major effector of 5-HT_{7R}, as most of the transcriptional actions of 5-HT_{7R} engagement by 5-HT can be abolished by PKA inhibitors and mimicked by PKA activators. Furthermore, the connexion between 5-HT_{7R} and PKA activation fits well with the global anti-inflammatory skewing induced by 5-HT via 5-HT_{7R} because PKA leads to CREB activation, which favours the acquisition of a “M2 polarization state”⁶². In addition, cAMP-initiated signaling limits the effector functions of pro-inflammatory stimuli^{85,86}, which is consistent with the reduced production of proinflammatory cytokines seen with 5-HT_{7R} activation.

The ability of 5-HT to promote the acquisition of a pro-fibrotic and anti-inflammatory signature in human macrophages has relevant pathophysiological implications. While normal peripheral blood levels of 5-HT range between 0.7 and 2.5 μM ^{87–91}, 5-HT concentrations at the neuronal synapse have been estimated to reach the millimolar range⁹², and the available platelet serotonin is close to 20 μM ⁹³. Since platelets release serotonin during inflammation as a means to activate endothelial cells and promote leukocyte adhesion and recruitment⁹³, our findings on the macrophage polarizing effects of 10 μM 5-HT are physiologically relevant, especially at the initial stages of inflammatory responses. Besides, and regarding pathology, the serum levels of 5-HT detected in metastatic carcinoid tumors exceed 30 μM ⁹¹, thus pointing to 5-HT as a factor that contributes to polarization of macrophages in serotonin-producing neuroendocrine tumors. Therefore, 5HT_{7R}-regulated genes should be considered as potential targets to modify macrophage polarization under pathological settings.

Materials and Methods

Ethical statement. Ethical approvals for all blood sources and processes used in this study have been approved by the Centro de Investigaciones Biológicas Ethics Committees. Subjects gave written informed consent in accordance to the Declaration of Helsinki. All experiments were carried out in accordance with the approved guidelines and regulations.

All experiments on mice were conducted according to the Spanish and European regulations on care and protection of laboratory animals and were approved by the Consejo Superior de Investigaciones Científicas ethics committee.

Generation of human monocyte-derived macrophages and cell isolation and culture. Human peripheral blood mononuclear cells (PBMC) were isolated from buffy coats from normal donors over a Lymphoprep (Nycomed Pharma, Oslo, Norway) gradient according to standard procedures. Monocytes were purified from PBMC by magnetic cell sorting using CD14 microbeads (Miltenyi Biotec, Bergisch Gladbach, Germany). Monocytes (>95% CD14⁺ cells) were cultured at 0.5×10^6 cells/ml for 7 days in RMI supplemented with 10% fetal calf serum (FCS) (completed medium), at 37 °C in a humidified atmosphere with 5% CO₂, and containing M-CSF (10 ng/ml) (ImmunoTools GmbH, Friesoythe, Germany) to generate monocyte-derived macrophages (M-MØ). Cytokine was added every two days. Before treatment with 5HT, M-MØ macrophages were maintained in serum-free medium for 48 hours, without a significant change in the level of expression of M-MØ-specific markers. Macrophage activation was accomplished with either ultrapure LPS (*E. coli* 055:B5, 10 ng/ml, Invivogen, San Diego, CA), synthetic triacylated lipoprotein (Pam3CSK4, 10 $\mu\text{g}/\text{ml}$, Invivogen) or IFN γ (10–100 IU/ml, Miltenyi Biotec). Bone marrow-derived mouse macrophages were also generated using GM-CSF (mouse GM-MØ) or M-CSF (mouse M-MØ) as described previously^{94,95}. RNA from mouse liver cells was obtained as previously described⁴⁴. Isolation of mouse peritoneal mouse macrophages was done by magnetic cell sorting using F4/80-biotin and Streptavidin microbeads (Miltenyi Biotec). For activation, macrophages were treated with *Escherichia coli* 055:B5 LPS (100 ng/ml for mouse macrophages; 10 ng/ml for human macrophages) for 24 h. 5-HT was obtained from Sigma Aldrich and used at 10 μM . 5-HT_{7R} agonists AS19 was obtained from Tocris Bioscience and used at 1 μM . 5-HT_{7R} antagonists (SB269970 and SB258719) were purchased from Sigma Aldrich and Tocris Bioscience, respectively, and added at 10 μM 1 hour before 5-HT treatment. cAMP analogues (BrcAMP and dBrcAMP) were used at 200 μM and 50 μM , respectively. The PKA activator 6BNZ-cAMP (6Bnz) and the EPAC-specific activator 8-pCPT-2'-O-Me-cAMP (8cPT) were obtained from Sigma Aldrich and used at 200 μM and 100 μM , respectively. The PKA-specific inhibitor RP-8-CPT-cAMPs (RP8) was obtained from Biolog and used at 100 μM .

ELISA. Culture supernatants from untreated or LPS-treated (24 h) human macrophages were assayed for the presence of cytokines using commercially available ELISA for human TNF α , IL-12p40 (BD Pharmingen), CXCL10, IL-10 (Biolegend), activin A and TGF β (R&D Systems). ELISA was performed following the protocols supplied by the manufacturers.

Quantitative real-time RT-PCR. Oligonucleotides for selected genes were designed according to the Universal Probe Roche library system (Roche Diagnostics) for quantitative real time PCR (qRT-PCR). Total RNA was extracted using the RNeasy kit (Qiagen), retrotranscribed, and amplified in triplicates. Results were expressed relative to the expression level of *TBP* RNA. When indicated, results were expressed relative to the mean of the expression level of endogenous reference genes *HPRT1*, *TBP* and *RPLP0*. In all cases the results were expressed using the $\Delta\Delta\text{CT}$ method for quantitation.

Microarray analysis. Global gene expression analysis was performed on RNA obtained from untreated or 5-HT-treated (10 μM , 6 h) M-MØ from three independent healthy donors. RNA was isolated using the RNeasy Mini kit (Qiagen, Germantown, MD) and labeled RNA used as a hybridization probe on Whole Human Genome Microarrays (Agilent Technologies, Palo Alto, CA). Only probes with signal values > 60% quantile in at least one condition were considered for the differential expression and statistical analysis. Statistical analysis for differential gene expression was carried out using empirical Bayes moderated t test implemented in the limma package (<http://www.bioconductor.org>). The p values were further adjusted for multiple hypotheses testing using the

Benjamini-Hochberg method to control the false discovery rate⁹⁶. All the above procedures were coded in R (<http://www.r-project.org>). Microarray data were deposited in the Gene Expression Omnibus (<http://www.ncbi.nlm.nih.gov/geo/>) under accession GSE94608. Differentially expressed genes were analysed for annotated gene sets enrichment using the online tool ENRICH (<http://amp.pharm.mssm.edu/Enrichr/>)^{97,98}. Enrichment terms were considered significant when they had a Benjamini-Hochberg-adjusted *p* value < 0.05. For gene set enrichment analysis (GSEA)⁹⁹, the gene sets contained in the Molecular Signature databases available at the GSEA website, and the previously defined “Pro-inflammatory gene set” and “Anti-inflammatory gene set”⁴⁸, which contain the top and bottom 150 probes from the GM-MØ versus M-MØ limma analysis of the microarray data in GSE68061 (ranked on the basis of the value of the *t* statistic), were used.

Western blot. Cell lysates were obtained in RIPA buffer (10 mM Tris-HCl pH 8, 150 mM NaCl, 1% NP-40, 2 mM Pefabloc, 2 mg/ml aprotinin/antipain/leupeptin/pepstatin, 10 mM NaF, and 1 mM Na₃VO₄). 20 µg of cell lysate was subjected to SDS-PAGE and transferred onto an Immobilon polyvinylidene difluoride membrane (Millipore). Protein detection was carried out using antibodies against phosphorylated STAT1 (BD Biosciences, CA, USA) and a monoclonal antibody against GAPDH (sc-32233, Santa Cruz, CA, USA).

Bleomycin-induced skin fibrosis mouse model. Skin fibrosis was induced in 6–8 week-old, pathogen-free WT or *Htr7*^{-/-100} female C57BL/6NJ (The Jackson Laboratory) by subcutaneous injections of 100 µg of bleomycin (1 mg/ml, Mylan Pharmaceuticals, Barcelona, Spain) or 0.9% saline control into the shaved back skin every day for 4 weeks as previously described^{61,101}. Skin was harvested and frozen for mRNA/protein studies or paraffin embedded for histological studies. Fibrosis was determined by Masson’s trichrome staining, and the presence of α-SMA⁺ or F4/80⁺ determined using anti-α Smooth Muscle Actin antibody (α-SMA; 1A4 clone, Sigma-Aldrich, Spain) and anti-F4/80 antibody (BM8 clone; eBioscience, San Diego, CA, USA).

Statistical analysis. For comparison of means, and unless otherwise indicated, statistical significance of the generated data was evaluated using the Student *t* test. In all cases, *p* < 0.05 was considered as statistically significant.

Data Availability. All data generated or analysed during this study are included in this published article. Moreover, microarray data were deposited in the Gene Expression Omnibus (<http://www.ncbi.nlm.nih.gov/geo/>) under accession GSE94608.

References

- Lesurtel, M., Soll, C., Graf, R. & Clavien, P. A. Role of serotonin in the hepato-gastrointestinal tract: an old molecule for new perspectives. *Cell Mol Life Sci* **65**, 940–952 (2008).
- Amireault, P., Sibon, D. & Cote, F. Life without peripheral serotonin: insights from tryptophan hydroxylase 1 knockout mice reveal the existence of paracrine/autocrine serotonergic networks. *ACS Chem Neurosci* **4**, 64–71, <https://doi.org/10.1021/cn300154j> (2013).
- Berger, M., Gray, J. A. & Roth, B. L. The expanded biology of serotonin. *Annu Rev Med* **60**, 355–366, <https://doi.org/10.1146/annurev.med.60.042307.110802> (2009).
- Kaumann, A. J. & Levy, F. O. 5-hydroxytryptamine receptors in the human cardiovascular system. *Pharmacology & therapeutics* **111**, 674–706 (2006).
- Spiller, R. Serotonin and GI clinical disorders. *Neuropharmacology* **55**, 1072–1080, <https://doi.org/10.1016/j.neuropharm.2008.07.016> (2008).
- Yano, J. M. *et al.* Indigenous bacteria from the gut microbiota regulate host serotonin biosynthesis. *Cell* **161**, 264–276, <https://doi.org/10.1016/j.cell.2015.02.047> (2015).
- Nemecek, G. M., Coughlin, S. R., Handley, D. A. & Moskowitz, M. A. Stimulation of aortic smooth muscle cell mitogenesis by serotonin. *Proceedings of the National Academy of Sciences of the United States of America* **83**, 674–678 (1986).
- Lesurtel, M. *et al.* Platelet-derived serotonin mediates liver regeneration. *Science* **312**, 104–107 (2006).
- Pakala, R., Willerson, J. T. & Benedict, C. R. Mitogenic effect of serotonin on vascular endothelial cells. *Circulation* **90**, 1919–1926 (1994).
- Barnes, N. M. & Sharp, T. A review of central 5-HT receptors and their function. *Neuropharmacology* **38**, 1083–1152 (1999).
- Ahern, G. P. 5-HT and the immune system. *Curr Opin Pharmacol* **11**, 29–33.
- Leon-Ponte, M., Ahern, G. P. & O’Connell, P. J. Serotonin provides an accessory signal to enhance T-cell activation by signaling through the 5-HT₇ receptor. *Blood* **109**, 3139–3146 (2007).
- Arzt, E., Costas, M., Finkielman, S. & Nahmod, V. E. Serotonin inhibition of tumor necrosis factor-α synthesis by human monocytes. *Life sciences* **48**, 2557–2562 (1991).
- Cloez-Tayarani, I., Petit-Bertron, A. F., Venters, H. D. & Cavaillon, J. M. Differential effect of serotonin on cytokine production in lipopolysaccharide-stimulated human peripheral blood mononuclear cells: involvement of 5-hydroxytryptamine_{2A} receptors. *International immunology* **15**, 233–240 (2003).
- Durk, T. *et al.* 5-Hydroxytryptamine modulates cytokine and chemokine production in LPS-primed human monocytes via stimulation of different 5-HTR subtypes. *International immunology* **17**, 599–606 (2005).
- Menard, G., Turmel, V. & Bissonnette, E. Y. Serotonin modulates the cytokine network in the lung: involvement of prostaglandin E₂. *Clinical and experimental immunology* **150**, 340–348 (2007).
- Launay, J. M. *et al.* Serotonin 5-HT_{2B} receptors are required for bone-marrow contribution to pulmonary arterial hypertension. *Blood* **119**, 1772–1780, <https://doi.org/10.1182/blood-2011-06-358374> (2012).
- Morita, T. *et al.* HTR₇ Mediates Serotonergic Acute and Chronic Itch. *Neuron* **87**, 124–138, <https://doi.org/10.1016/j.neuron.2015.05.044> (2015).
- Dees, C. *et al.* Platelet-derived serotonin links vascular disease and tissue fibrosis. *The Journal of experimental medicine* **208**, 961–972, <https://doi.org/10.1084/jem.20101629> (2011).
- Kim, J. J. & Khan, W. I. 5-HT₇ receptor signaling: improved therapeutic strategy in gut disorders. *Front Behav Neurosci* **8**, 396, <https://doi.org/10.3389/fnbeh.2014.00396> (2014).
- Levin, A. D. & van den Brink, G. R. Selective inhibition of mucosal serotonin as treatment for IBD? *Gut* **63**, 866–867, <https://doi.org/10.1136/gutjnl-2013-305283> (2014).
- Kim, J. J. *et al.* Targeted inhibition of serotonin type 7 (5-HT₇) receptor function modulates immune responses and reduces the severity of intestinal inflammation. *J Immunol* **190**, 4795–4804, <https://doi.org/10.4049/jimmunol.1201887> (2013).

23. Guseva, D. *et al.* Serotonin 5-HT₇ receptor is critically involved in acute and chronic inflammation of the gastrointestinal tract. *Inflamm Bowel Dis* **20**, 1516–1529, <https://doi.org/10.1097/MIB.000000000000150> (2014).
24. Ghia, J. E. *et al.* Serotonin has a key role in pathogenesis of experimental colitis. *Gastroenterology* **137**, 1649–1660, <https://doi.org/10.1053/j.gastro.2009.08.041> (2009).
25. Li, N. *et al.* Serotonin activates dendritic cell function in the context of gut inflammation. *The American journal of pathology* **178**, 662–671, <https://doi.org/10.1016/j.ajpath.2010.10.028> (2011).
26. Nocito, A. *et al.* Serotonin regulates macrophage-mediated angiogenesis in a mouse model of colon cancer allografts. *Cancer research* **68**, 5152–5158 (2008).
27. Svejda, B. *et al.* Serotonin and the 5-HT₇ receptor: the link between hepatocytes, IGF-1 and small intestinal neuroendocrine tumors. *Cancer Sci* **104**, 844–855, <https://doi.org/10.1111/cas.12174> (2013).
28. Chabbi-Achengli, Y. *et al.* Serotonin Is Involved in Autoimmune Arthritis through Th17 Immunity and Bone Resorption. *The American journal of pathology* **186**, 927–937, <https://doi.org/10.1016/j.ajpath.2015.11.018> (2016).
29. Shajib, M. S. & Khan, W. I. The role of serotonin and its receptors in activation of immune responses and inflammation. *Acta Physiol (Oxf)* **213**, 561–574, <https://doi.org/10.1111/apha.12430> (2015).
30. Nazimek, K. *et al.* The role of macrophages in anti-inflammatory activity of antidepressant drugs. *Immunobiology*, <https://doi.org/10.1016/j.imbio.2016.07.001> (2016).
31. Su, H. C. *et al.* Glycogen synthase kinase-3 β regulates anti-inflammatory property of fluoxetine. *Int Immunopharmacol* **14**, 150–156, <https://doi.org/10.1016/j.intimp.2012.06.015> (2012).
32. Tsuchida, Y. *et al.* Neuronal stimulation with 5-hydroxytryptamine 4 receptor induces anti-inflammatory actions via α 7nACh receptors on muscularis macrophages associated with postoperative ileus. *Gut* **60**, 638–647, <https://doi.org/10.1136/gut.2010.227546> (2011).
33. Maehara, T. *et al.* Therapeutic action of 5-HT₃ receptor antagonists targeting peritoneal macrophages in post-operative ileus. *British journal of pharmacology* **172**, 1136–1147, <https://doi.org/10.1111/bph.13006> (2015).
34. Jantsch, J., Binger, K. J., Muller, D. N. & Titzel, J. Macrophages in homeostatic immune function. *Frontiers in physiology* **5**, 146, <https://doi.org/10.3389/fphys.2014.00146> (2014).
35. Sica, A. & Mantovani, A. Macrophage plasticity and polarization: *in vivo* veritas. *The Journal of clinical investigation* **122**, 787–795, <https://doi.org/10.1172/JCI59643> (2012).
36. Martinez, F. O., Sica, A., Mantovani, A. & Locati, M. Macrophage activation and polarization. *Front Biosci* **13**, 453–461 (2008).
37. Schultze, J. L. Reprogramming of macrophages—new opportunities for therapeutic targeting. *Current opinion in pharmacology* **26**, 10–15, <https://doi.org/10.1016/j.coph.2015.09.007> (2016).
38. Schultze, J. L., Freeman, T., Hume, D. A. & Latz, E. A transcriptional perspective on human macrophage biology. *Seminars in immunology* **27**, 44–50, <https://doi.org/10.1016/j.smim.2015.02.001> (2015).
39. Kalkman, H. O. & Feuerbach, D. Antidepressant therapies inhibit inflammation and microglial M1-polarization. *Pharmacology & therapeutics* **163**, 82–93, <https://doi.org/10.1016/j.pharmthera.2016.04.001> (2016).
40. Verreck, F. A. *et al.* Human IL-23-producing type 1 macrophages promote but IL-10-producing type 2 macrophages subvert immunity to (myco)bacteria. *Proceedings of the National Academy of Sciences of the United States of America* **101**, 4560–4565, <https://doi.org/10.1073/pnas.0400983101> (2004).
41. Li, G., Kim, Y. J. & Broxmeyer, H. E. Macrophage colony-stimulating factor drives cord blood monocyte differentiation into IL-10(high)IL-12absent dendritic cells with tolerogenic potential. *J Immunol* **174**, 4706–4717 (2005).
42. Akagawa, K. S. Functional heterogeneity of colony-stimulating factor-induced human monocyte-derived macrophages. *Int J Hematol* **76**, 27–34 (2002).
43. Hamilton, J. A. Colony-stimulating factors in inflammation and autoimmunity. *Nature reviews. Immunology* **8**, 533–544 (2008).
44. de las Casas-Engel, M. *et al.* Serotonin skews human macrophage polarization through HTR2B and HTR7. *Journal of immunology* **190**, 2301–2310, <https://doi.org/10.4049/jimmunol.1201133> (2013).
45. Roth, B. L. Drugs and valvular heart disease. *The New England journal of medicine* **356**, 6–9, <https://doi.org/10.1056/NEJMp068265> (2007).
46. Schade, R., Andersohn, F., Suissa, S., Haverkamp, W. & Garbe, E. Dopamine agonists and the risk of cardiac-valve regurgitation. *The New England journal of medicine* **356**, 29–38, <https://doi.org/10.1056/NEJMoa062222> (2007).
47. Cuevas, V. D. *et al.* MAFB Determines Human Macrophage Anti-Inflammatory Polarization: Relevance for the Pathogenic Mechanisms Operating in Multicentric Carpotalarsal Osteolysis. *J Immunol*, <https://doi.org/10.4049/jimmunol.1601667> (2017).
48. Gonzalez-Dominguez, E. *et al.* Atypical Activin A and IL-10 Production Impairs Human CD16+ Monocyte Differentiation into Anti-Inflammatory Macrophages. *J Immunol* **196**, 1327–1337, <https://doi.org/10.4049/jimmunol.1501177> (2016).
49. Sierra-Filardi, E. *et al.* Activin A skews macrophage polarization by promoting a proinflammatory phenotype and inhibiting the acquisition of anti-inflammatory macrophage markers. *Blood* **117**, 5092–5101 (2011).
50. Lovell, P. J. *et al.* A novel, potent, and selective 5-HT₇ antagonist: (R)-3-(2-(2-(4-methylpiperidin-1-yl)ethyl)pyrrolidine-1-sulfonyl) phenol (SB-269970). *J Med Chem* **43**, 342–345 (2000).
51. Pouzet, B. SB-258741: a 5-HT₇ receptor antagonist of potential clinical interest. *CNS Drug Rev* **8**, 90–100 (2002).
52. Forbes, I. T., Jones, G. E., Murphy, O. E., Holland, V. & Baxter, G. S. N-(1-methyl-5-indolyl)-N'-(3-methyl-5-isothiazolyl)urea: a novel, high-affinity 5-HT_{2B} receptor antagonist. *J Med Chem* **38**, 855–857 (1995).
53. Raymond, J. R. *et al.* Multiplicity of mechanisms of serotonin receptor signal transduction. *Pharmacology & therapeutics* **92**, 179–212 (2001).
54. Wynn, T. A. & Vannella, K. M. Macrophages in Tissue Repair, Regeneration, and Fibrosis. *Immunity* **44**, 450–462, <https://doi.org/10.1016/j.immuni.2016.02.015> (2016).
55. Munoz-Canoves, P. & Serrano, A. L. Macrophages decide between regeneration and fibrosis in muscle. *Trends Endocrinol Metab* **26**, 449–450, <https://doi.org/10.1016/j.tem.2015.07.005> (2015).
56. Christmann, R. B. *et al.* Association of Interferon- and transforming growth factor β -regulated genes and macrophage activation with systemic sclerosis-related progressive lung fibrosis. *Arthritis Rheumatol* **66**, 714–725, <https://doi.org/10.1002/art.38288> (2014).
57. Stifano, G. *et al.* Chronic Toll-like receptor 4 stimulation in skin induces inflammation, macrophage activation, transforming growth factor β signature gene expression, and fibrosis. *Arthritis Res Ther* **16**, R136, <https://doi.org/10.1186/ar4598> (2014).
58. Murray, L. A. *et al.* TGF- β driven lung fibrosis is macrophage dependent and blocked by Serum amyloid P. *The international journal of biochemistry & cell biology* **43**, 154–162, <https://doi.org/10.1016/j.biocel.2010.10.013> (2011).
59. Murray, L. A. *et al.* Serum amyloid P therapeutically attenuates murine bleomycin-induced pulmonary fibrosis via its effects on macrophages. *PloS one* **5**, e9683, <https://doi.org/10.1371/journal.pone.0009683> (2010).
60. Lemos, D. R. *et al.* Nilotinib reduces muscle fibrosis in chronic muscle injury by promoting TNF-mediated apoptosis of fibro/adipogenic progenitors. *Nature medicine* **21**, 786–794, <https://doi.org/10.1038/nm.3869> (2015).
61. Yamamoto, T. Animal model of systemic sclerosis. *J Dermatol* **37**, 26–41, <https://doi.org/10.1111/j.1346-8138.2009.00764.x> (2010).
62. Ruffell, D. *et al.* A CREB-C/EBP β cascade induces M2 macrophage-specific gene expression and promotes muscle injury repair. *Proceedings of the National Academy of Sciences of the United States of America* **106**, 17475–17480 (2009).
63. Lumeng, C. N., Bodzin, J. L. & Saltiel, A. R. Obesity induces a phenotypic switch in adipose tissue macrophage polarization. *The Journal of clinical investigation* **117**, 175–184 (2007).

64. Ruffell, B. & Coussens, L. M. Macrophages and therapeutic resistance in cancer. *Cancer Cell* **27**, 462–472, <https://doi.org/10.1016/j.ccell.2015.02.015> (2015).
65. Gordon, S. & Martinez, F. O. Alternative activation of macrophages: mechanism and functions. *Immunity* **32**, 593–604 (2010).
66. Mantovani, A., Biswas, S. K., Galdiero, M. R., Sica, A. & Locati, M. Macrophage plasticity and polarization in tissue repair and remodelling. *The Journal of pathology* **229**, 176–185, <https://doi.org/10.1002/path.4133> (2013).
67. Jaffre, F. *et al.* Involvement of the serotonin 5-HT_{2B} receptor in cardiac hypertrophy linked to sympathetic stimulation: control of interleukin-6, interleukin-1beta, and tumor necrosis factor-alpha cytokine production by ventricular fibroblasts. *Circulation* **110**, 969–974 (2004).
68. Nebigil, C. G. *et al.* Overexpression of the serotonin 5-HT_{2B} receptor in heart leads to abnormal mitochondrial function and cardiac hypertrophy. *Circulation* **107**, 3223–3229 (2003).
69. Elangbam, C. S. Drug-induced valvulopathy: an update. *Toxicol Pathol* **38**, 837–848, <https://doi.org/10.1177/0192623310378027> (2010).
70. Puig-Kroger, A. *et al.* Folate receptor beta is expressed by tumor-associated macrophages and constitutes a marker for M2 anti-inflammatory/regulatory macrophages. *Cancer research* **69**, 9395–9403 (2009).
71. Li, H., Nagai, T., Hasui, K. & Matsuyama, T. Depletion of folate receptor beta-expressing macrophages alleviates bleomycin-induced experimental skin fibrosis. *Mod Rheumatol* **24**, 816–822, <https://doi.org/10.3109/14397595.2013.879415> (2014).
72. Holst, K. *et al.* The serotonin receptor 5-HT₇R regulates the morphology and migratory properties of dendritic cells. *Journal of cell science* **128**, 2866–2880, <https://doi.org/10.1242/jcs.167999> (2015).
73. Polat, B. *et al.* Liver 5-HT₇ receptors: A novel regulator target of fibrosis and inflammation-induced chronic liver injury *in vivo* and *in vitro*. *Int Immunopharmacol* **43**, 227–235, <https://doi.org/10.1016/j.intimp.2016.12.023> (2017).
74. Gellynck, E. *et al.* The serotonin 5-HT₇ receptors: two decades of research. *Exp Brain Res* **230**, 555–568, <https://doi.org/10.1007/s00221-013-3694-y> (2013).
75. Bard, J. A. *et al.* Cloning of a novel human serotonin receptor (5-HT₇) positively linked to adenylate cyclase. *The Journal of biological chemistry* **268**, 23422–23426 (1993).
76. Tuladhar, B. R., Ge, L. & Naylor, R. J. 5-HT₇ receptors mediate the inhibitory effect of 5-HT on peristalsis in the isolated guinea-pig ileum. *British journal of pharmacology* **138**, 1210–1214, <https://doi.org/10.1038/sj.bjp.0705184> (2003).
77. Idzko, M. *et al.* The serotonergic receptors of human dendritic cells: identification and coupling to cytokine release. *Journal of immunology* **172**, 6011–6019 (2004).
78. Soga, F., Katoh, N., Inoue, T. & Kishimoto, S. Serotonin activates human monocytes and prevents apoptosis. *The Journal of investigative dermatology* **127**, 1947–1955, <https://doi.org/10.1038/sj.jid.5700824> (2007).
79. Norum, J. H., Hart, K. & Levy, F. O. Ras-dependent ERK activation by the human G(s)-coupled serotonin receptors 5-HT₄(b) and 5-HT₇(a). *The Journal of biological chemistry* **278**, 3098–3104, <https://doi.org/10.1074/jbc.M206237200> (2003).
80. Johnson-Farley, N. N., Kertesz, S. B., DUBYAK, G. R. & Cowen, D. S. Enhanced activation of Akt and extracellular-regulated kinase pathways by simultaneous occupancy of Gq-coupled 5-HT_{2A} receptors and Gs-coupled 5-HT_{7A} receptors in PC12 cells. *J Neurochem* **92**, 72–82, <https://doi.org/10.1111/j.1471-4159.2004.02832.x> (2005).
81. Lieb, K. *et al.* Serotonin via 5-HT₇ receptors activates p38 mitogen-activated protein kinase and protein kinase C epsilon resulting in interleukin-6 synthesis in human U373 MG astrocytoma cells. *J Neurochem* **93**, 549–559, <https://doi.org/10.1111/j.1471-4159.2005.03079.x> (2005).
82. Kvachina, E. *et al.* 5-HT₇ receptor is coupled to G alpha subunits of heterotrimeric G12-protein to regulate gene transcription and neuronal morphology. *J Neurosci* **25**, 7821–7830, <https://doi.org/10.1523/JNEUROSCI.1790-05.2005> (2005).
83. Renner, U. *et al.* Heterodimerization of serotonin receptors 5-HT_{1A} and 5-HT₇ differentially regulates receptor signalling and trafficking. *Journal of cell science* **125**, 2486–2499, <https://doi.org/10.1242/jcs.101337> (2012).
84. Guseva, D., Wirth, A. & Ponimaskin, E. Cellular mechanisms of the 5-HT₇ receptor-mediated signaling. *Front Behav Neurosci* **8**, 306, <https://doi.org/10.3389/fnbeh.2014.00306> (2014).
85. Shirshov, S. V. Role of Epac proteins in mechanisms of cAMP-dependent immunoregulation. *Biochemistry (Mosc)* **76**, 981–998, <https://doi.org/10.1134/S000629791109001X> (2011).
86. Peters-Golden, M. Putting on the brakes: cyclic AMP as a multipronged controller of macrophage function. *Sci Signal* **2**, pe37, <https://doi.org/10.1126/scisignal.275pe37> (2009).
87. Lieder, H. R., Baars, T., Kahlert, P. & Kleinbongard, P. Aspirate from human stented saphenous vein grafts induces epicardial coronary vasoconstriction and impairs perfusion and left ventricular function in rat bioassay hearts with pharmacologically induced endothelial dysfunction. *Physiol Rep* **4**, <https://doi.org/10.14814/phy2.12874> (2016).
88. Chojnacki, C. *et al.* Serum and ascitic fluid serotonin levels and 5-hydroxyindoleacetic acid urine excretion in the liver of cirrhotic patients with encephalopathy. *Adv Med Sci* **58**, 251–256, <https://doi.org/10.2478/ams-2013-0010> (2013).
89. Abid, S. *et al.* Inhibition of gut- and lung-derived serotonin attenuates pulmonary hypertension in mice. *American journal of physiology* **303**, L500–508, <https://doi.org/10.1152/ajplung.00049.2012> (2012).
90. Comai, S. *et al.* Serum levels of tryptophan, 5-hydroxytryptophan and serotonin in patients affected with different forms of amenorrhea. *Int J Tryptophan Res* **3**, 69–75 (2010).
91. Onaitis, M. W. *et al.* Gastrointestinal carcinoids: characterization by site of origin and hormone production. *Ann Surg* **232**, 549–556 (2000).
92. Bunin, M. A. & Wightman, R. M. Quantitative evaluation of 5-hydroxytryptamine (serotonin) neuronal release and uptake: an investigation of extrasynaptic transmission. *J Neurosci* **18**, 4854–4860 (1998).
93. Duerschmied, D. *et al.* Platelet serotonin promotes the recruitment of neutrophils to sites of acute inflammation in mice. *Blood* **121**, 1008–1015, <https://doi.org/10.1182/blood-2012-06-437392> (2013).
94. Fleetwood, A. J., Dinh, H., Cook, A. D., Hertzog, P. J. & Hamilton, J. A. GM-CSF- and M-CSF-dependent macrophage phenotypes display differential dependence on type I interferon signaling. *Journal of leukocyte biology* **86**, 411–421 (2009).
95. Fleetwood, A. J., Lawrence, T., Hamilton, J. A. & Cook, A. D. Granulocyte-macrophage colony-stimulating factor (CSF) and macrophage CSF-dependent macrophage phenotypes display differences in cytokine profiles and transcription factor activities: implications for CSF blockade in inflammation. *Journal of immunology* **178**, 5245–5252 (2007).
96. Hochberg, Y. & Benjamini, Y. More powerful procedures for multiple significance testing. *Stat Med* **9**, 811–818 (1990).
97. Kuleshov, M. V. *et al.* Enrichr: a comprehensive gene set enrichment analysis web server 2016 update. *Nucleic acids research* **44**, W90–W97, <https://doi.org/10.1093/nar/gkw377> (2016).
98. Chen, E. Y. *et al.* Enrichr: interactive and collaborative HTML5 gene list enrichment analysis tool. *BMC Bioinformatics* **14**, 128, <https://doi.org/10.1186/1471-2105-14-128> (2013).
99. Subramanian, A. *et al.* Gene set enrichment analysis: a knowledge-based approach for interpreting genome-wide expression profiles. *Proceedings of the National Academy of Sciences of the United States of America* **102**, 15545–15550, <https://doi.org/10.1073/pnas.0506580102> (2005).
100. Hedlund, P. B. *et al.* No hypothermic response to serotonin in 5-HT₇ receptor knockout mice. *Proceedings of the National Academy of Sciences of the United States of America* **100**, 1375–1380, <https://doi.org/10.1073/pnas.0337340100> (2003).
101. Usategui, A., Criado, G., Del Rey, M. J., Fare, R. & Pablos, J. L. Topical vitamin D analogue calcipotriol reduces skin fibrosis in experimental scleroderma. *Arch Dermatol Res* **306**, 757–761, <https://doi.org/10.1007/s00403-014-1466-6> (2014).

Acknowledgements

This work was supported by grants from Ministerio de Economía y Competitividad (SAF2011-23801 and SAF2014-52423-R to MAV and ALC, and PI I12/439 to JLP), “Programa de Actividades de I + D” from the Comunidad de Madrid/FEDER (RAPHYME S2010/BMD-2350 to JLP and ALC), and RIER (Red de Investigación en Inflamación y Enfermedades Reumáticas, RD12/09 to ALC and JLP) from the Instituto de Salud Carlos III, Ministerio de Economía y Competitividad, Spain (co-financed by FEDER, European Union). MCE was supported by an FPI predoctoral fellowship (BES-2009-021465) from Ministerio de Economía e Innovación.

Author Contributions

A.D.S., M.C.E., M.S.F., A.U., C.N. and V.D.C. performed research; A.D.S., M.A.V., J.L.P. and A.L.C. designed the research; A.D.S. analyzed data and prepared figures; A.L.C. wrote the paper.

Additional Information

Supplementary information accompanies this paper at <https://doi.org/10.1038/s41598-017-15348-y>.

Competing Interests: The authors declare that they have no competing interests.

Publisher's note: Springer Nature remains neutral with regard to jurisdictional claims in published maps and institutional affiliations.



Open Access This article is licensed under a Creative Commons Attribution 4.0 International License, which permits use, sharing, adaptation, distribution and reproduction in any medium or format, as long as you give appropriate credit to the original author(s) and the source, provide a link to the Creative Commons license, and indicate if changes were made. The images or other third party material in this article are included in the article's Creative Commons license, unless indicated otherwise in a credit line to the material. If material is not included in the article's Creative Commons license and your intended use is not permitted by statutory regulation or exceeds the permitted use, you will need to obtain permission directly from the copyright holder. To view a copy of this license, visit <http://creativecommons.org/licenses/by/4.0/>.

© The Author(s) 2017